



Published in final edited form as:

Science. 2012 August 3; 337(6094): 587–590. doi:10.1126/science.1223560.

Mitochondrial Import Efficiency of ATFS-1 Regulates Mitochondrial UPR Activation

Amrita M. Nargund^{1,†}, Mark W. Pellegrino^{1,†}, Christopher J. Fiorese^{1,2}, Brooke M. Baker¹, and Cole M. Haynes^{1,2,*}

¹Cell Biology Program, Memorial Sloan-Kettering Cancer Center, New York, New York 10065, USA

²BCMB Allied Program, Weill Cornell Medical College, 1300 York Avenue, New York, New York, USA

Abstract

To better understand the response to mitochondrial dysfunction, we examined the mechanism by which Activating Transcription Factor associated with Stress-1 (ATFS-1) senses mitochondrial stress and communicates with the nucleus during the mitochondrial unfolded protein response (UPR^{mt}). We found that the key point of regulation was the mitochondrial import efficiency of ATFS-1. In addition to a nuclear localization sequence, ATFS-1 has an amino-terminal mitochondrial targeting sequence, which was essential for UPR^{mt} repression. Normally, ATFS-1 is imported into mitochondria and degraded. However, during mitochondrial stress, import efficiency was reduced allowing a percentage of ATFS-1 to accumulate in the cytosol and traffic to the nucleus. Our results show that cells monitor mitochondrial import efficiency via ATFS-1 to coordinate the level of mitochondrial dysfunction with the protective transcriptional response.

Mitochondria import ~99% of their proteome through the TOM (Translocase of the Outer Membrane) and TIM (Translocase of the Inner Membrane) complexes (1, 2). The mitochondrial protein-folding environment is maintained by mitochondrial molecular chaperones whose expression levels are coupled to the state of mitochondrial protein homeostasis by a mitochondria-to-nuclear signaling pathway termed the UPR^{mt} (3, 4). Evidence in *Caenorhabditis elegans* implicates the mitochondrial inner membrane peptide transporter, HAF-1, and the bZip transcription factor ATFS-1 in UPR^{mt} signaling (5).

During mitochondrial stress, ATFS-1 accumulates in the nucleus, because of a nuclear localization signal (NLS). A protein sequence prediction algorithm, Mitoprot II, predicted the presence of an amino-terminal mitochondrial targeting sequence (MTS) as well (6) (Fig. 1A). Indeed, amino acids 1-100 of ATFS-1 were sufficient to target green fluorescent protein (GFP) to HeLa cell mitochondria (Figs. 1B & S1). Consistent with cleavage of the MTS, the mitochondrial enriched form of ATFS-1¹⁻¹⁰⁰::GFP was smaller than the unprocessed form found in the postmitochondrial supernatant (Fig. 1C).

*To whom correspondence should be addressed. haynesc@mskcc.org.

†These authors contributed equally to this work.

Supplementary Materials

www.sciencemag.org

Materials and Methods

Figs. S1, S2, S3, S4, S5, S6, S7, S8, S9, S10, S11, S12, S13

References (16–22)

Tables S2, S3

To understand UPR^{mt} regulation in *C. elegans*, we sought to determine the localization of ATFS-1 in the absence of UPR^{mt}-activation. We were unable to detect endogenous ATFS-1 or the ATFS-1::GFP fusion protein using ATFS-1 or GFP-specific antibodies (Figs. 1D & S2). Additionally, *atfs-1_{pr}::gfp* worms expressed GFP strongly in all cells indicative of an active promoter, while the ATFS-1::GFP fusion protein was nearly undetectable (fig. S3A). These data suggest that ATFS-1 is rapidly degraded.

We hypothesized that ATFS-1 was degraded by a mitochondrial matrix protease such as the caseinolytic peptidase ClpP or Lon (7). Animals fed *lon*(RNAi), but not *clpp*(RNAi) accumulated endogenous ATFS-1 as well as ATFS-1::GFP (Figs. 1D, S3B & S3C). ATFS-1 was absent in lysates from *atfs-1(tm4525)* worms (Figs. 1D & S3D), which were unable to activate the UPR^{mt} (fig. S4). *lon*(RNAi) did not affect *atfs-1* transcription (fig. S5A). Furthermore, in *lon*(RNAi)-treated worms, ATFS-1 co-fractionated with a known mitochondrial protein (Figs. 1E & S3E). Unlike *spg-7*(RNAi), which impairs a mitochondrial protease required for electron transport chain (ETC) quality control and mitochondrial ribosome biogenesis (8), *lon*(RNAi) did not activate the UPR^{mt} transcriptional reporter *hsp-60_{pr}::gfp* or impair worm development (5) (Fig. 1F). Therefore, in the absence of UPR^{mt}-activation, ATFS-1 is imported into mitochondria and degraded.

During UPR^{mt} activation, ATFS-1::GFP accumulated in nuclei (Fig. 2A) (5). The predominant form of ATFS-1 that accumulated during *spg-7*(RNAi) or ethidium bromide (EtBr) treatment was of a higher molecular weight than the form detected in mitochondria of worms raised on *lon*(RNAi) and was enriched in the postmitochondrial supernatant (Figs. 2B & S4C) suggesting that during UPR^{mt} activation, a percentage of ATFS-1 remains in the cytosol, thus maintaining its MTS.

Mitochondrial toxins such as paraquat, which activated the UPR^{mt} (Fig. 3A), are known to impair mitochondrial import causing the accumulation of MTS containing proteins in the cytosol (9). To determine if a general impairment of import occurs during UPR^{mt} activation, we generated a transgenic strain expressing GFP with a MTS (GFP^{mt}) (10, 11). Because steady-state detection of unprocessed MTS containing proteins is very difficult (12), we expressed GFP^{mt} via the inducible *hsp-16* promoter (fig. S6). Only in the presence of UPR^{mt}-activating stress was unprocessed GFP^{mt} detected in the post-mitochondrial supernatant consistent with impaired import (Fig. 2C). Similarly, when ATFS-1 was expressed via the *hsp-16* promoter, unprocessed ATFS-1 was only detectable in the postmitochondrial supernatant during UPR^{mt}-activating stress (Figs. 2D & S6). Import was not completely blocked during UPR^{mt} activation because the processed forms of ATFS-1 (revealed by *lon*(RNAi)) and GFP^{mt} were detected in mitochondria (Figs. 2C & 2D).

Import into the matrix requires the TOM complex, the TIM23 complex, the ETC and the matrix-localized molecular chaperone mtHsp70 (1). *tim-23*(RNAi) caused ATFS-1::GFP to accumulate within nuclei (Fig. 2A) and strongly induced *hsp-60_{pr}::gfp* expression (Figs. 3A & S7). Furthermore, impairment of mtHsp70 (3) or the ETC by the *isp-1(qm150)* mutation (13) or *cco-1*(RNAi) also activated the UPR^{mt} suggesting that ATFS-1 responds to mitochondrial protein import perturbations (Fig. 3A).

We next considered how HAF-1, the previously identified UPR^{mt} regulator (5), affected ATFS-1. As expected, *haf-1(ok705)* worms were unable to induce *hsp-60_{pr}::gfp* expression caused by the *clk-1(qm30)* mutation (13) (Fig. 3B) or when raised on 30 μg/ml EtBr (Fig. 3A). However, *hsp-60_{pr}::gfp* induction caused by mitochondrial stresses that arrest worm development such as 100 μg/ml EtBr or *spg-7*(RNAi) treatment did not require *haf-1* (fig. S8). Additionally, UPR^{mt} activation caused by conditions that directly inhibited mitochondrial import such as *tomm-40*(RNAi) (fig. S8A), *tim-23*(RNAi), *cco-1*(RNAi) or

paraquat (9), also did not require *haf-1* (Fig. 3A), suggesting that HAF-1 affects UPR^{mt} signaling by modulating the mitochondrial import of ATFS-1. During mitochondrial stress, steady state measurements indicated that more ATFS-1 accumulated within mitochondria of *haf-1(ok705)* worms as revealed by *lon*(RNAi) (Figs. 3B & S6B). Thus, in the absence of *haf-1*, ATFS-1 partitions to mitochondria during stress reducing UPR^{mt} activation.

To more directly examine the effect of *haf-1(ok705)* on ATFS-1 mitochondrial import efficiency, ATFS-1 was expressed from the inducible *hsp-16* promoter (fig. S6). As discussed above, unprocessed ATFS-1 accumulated in the postmitochondrial supernatant during UPR^{mt}-activating stress. However, in *haf-1(ok705)* worms, much less ATFS-1 was detected in the cytosol (Fig. 2D). Similarly, the slowed import of GFP^{mt} during mitochondrial stress was not observed in *haf-1(ok705)* animals (Fig. 2C) suggesting that HAF-1 is a general attenuator of mitochondrial protein import during stress and is probably how HAF-1 modulates UPR^{mt} signaling.

To determine if prevention of ATFS-1 import into mitochondria is sufficient to cause ATFS-1 nuclear accumulation and UPR^{mt} activation, we generated a series of transgenic lines that expressed wild-type ATFS-1 (full-length (FL)), ATFS-1^{Δ1-32.myc}, an engineered variant of ATFS-1 unable to be imported into mitochondria, and ATFS-1^{Δ1-32.mycΔNLS} which lacked the NLS (fig. S9). Removal of the MTS was sufficient to cause nuclear accumulation of ATFS-1^{Δ1-32.myc::GFP} (Fig. 2A) and expression of ATFS-1^{Δ1-32.myc} caused constitutive expression of *hsp-60_{pr}::gfp* indicating that impaired mitochondrial import of ATFS-1 is sufficient for UPR^{mt} activation. Activation of *hsp-60_{pr}::gfp* by ATFS-1^{Δ1-32.myc} did not require *haf-1* (Fig. 3C) further supporting a role for HAF-1 in mitochondrial import regulation. Mutating the NLS in ATFS-1 lacking the MTS prevented *hsp-60_{pr}::gfp* expression indicating that when ATFS-1 cannot be imported into mitochondria, ATFS-1 requires the NLS for UPR^{mt} activation (Figs. 3C & 3D).

To examine the physiological role of ATFS-1 during mitochondrial dysfunction, wild-type, *clk-1(qm30)* or *isp-1(qm150)* (13) worms were raised on control or *atfs-1*(RNAi). While unstressed worms were unaffected by *atfs-1*(RNAi), the mitochondrial stressed worms were unable to develop (Figs. 4A & S13A). Because ATFS-1 is regulated by mitochondrial import efficiency, a process linked to mitochondrial function, we sought to identify the entire ATFS-1 mediated response. Transcripts from wild-type and *atfs-1(tm4525)* worms raised in the presence and absence of stress were compared. A broad transcriptional response totaling 685 genes was induced during mitochondrial stress (Fig. 4B & Table S2), of which 391 required *atfs-1* (Table S3).

Included in the ATFS-1 program were many genes with roles in protecting against mitochondrial dysfunction (Fig. 4C) including the mitochondrial chaperones *dnj-10* (14) (Fig. 4D) and *hsp-60* (Fig. S13B). Numerous components involved in reactive oxygen species detoxification required ATFS-1 for induction during stress including the transcription factor *skn-1* (15) (Fig. 4E). Several glycolysis genes including *gpd-2* (glyceraldehyde-3-phosphate dehydrogenase) were also induced (Fig. 4F) suggesting the UPR^{mt} may contribute to a shift in ATP production from respiration to glycolysis. ATFS-1 was also required for the induction of *tim-23* and *tim-17* (Figs. 4G & S13C); core components of the TIM23 complex (1).

The presence of a NLS and a MTS in a single transcriptional activator allows the cell to monitor global mitochondrial import efficiency and determine the level of mitochondrial dysfunction. If mitochondria are functioning properly the constitutively synthesized ATFS-1 partitions into mitochondria where it is degraded. As mitochondrial dysfunction increases, mitochondrial import efficiency is reduced favoring translocation of ATFS-1 to the nucleus.

Thus, mitochondrial homeostasis is maintained by the stress-dependent partitioning of a transcriptional activator between an inactive state in mitochondria and an active state in the nucleus.

Supplementary Material

Refer to Web version on PubMed Central for supplementary material.

Acknowledgments

This work was supported by the Louis V. Gerstner, Jr. Young Investigators Fund, the Alfred W. Bressler Scholar Fund, the Ellison Medical Foundation and the NIH (R01AG040061). We thank Kelly Rainbolt for *Ior1*(RNAi) advice, the National BioResource Project, the CGC and the Genomics Facility at MSKCC. The microarray data have been submitted in MIAME-compliant format to the Gene Expression Omnibus database (accession number GSE38196).

References and Notes

1. Chacinska A, Koehler CM, Milenkovic D, Lithgow T, Pfanner N. Importing mitochondrial proteins: machineries and mechanisms. *Cell*. 2009; 138(4):628.10.1016/j.cell.2009.08.005 [PubMed: 19703392]
2. Donzeau M, Kaldi K, Adam A, Paschen S, Wanner G, Guiard B, et al. Tim23 links the inner and outer mitochondrial membranes. *Cell*. 2000; 101(4):401. [PubMed: 10830167]
3. Yoneda T, Benedetti C, Urano F, Clark SG, Harding HP, Ron D. Compartment-specific perturbation of protein handling activates genes encoding mitochondrial chaperones. *J Cell Sci*. 2004; 117(Pt 18):4055.10.1242/jcs.01275 [PubMed: 15280428]
4. Zhao Q, Wang J, Levichkin IV, Stasinopoulos S, Ryan MT, Hoogenraad NJ. A mitochondrial specific stress response in mammalian cells. *Embo J*. 2002; 21(17):4411. [PubMed: 12198143]
5. Haynes CM, Yang Y, Blais SP, Neubert TA, Ron D. The matrix peptide exporter HAF-1 signals a mitochondrial UPR by activating the transcription factor ZC376.7 in *C. elegans*. *Mol Cell*. 2010; 37(4):529.10.1016/j.molcel.2010.01.015 [PubMed: 20188671]
6. Claros MG, Vincens P. Computational method to predict mitochondrially imported proteins and their targeting sequences. *Eur J Biochem*. 1996; 241(3):779. [PubMed: 8944766]
7. Tatsuta T, Langer T. Quality control of mitochondria: protection against neurodegeneration and ageing. *Embo J*. 2008; 27(2):306.10.1038/sj.emboj.7601972 [PubMed: 18216873]
8. Nolden M, Ehse S, Koppen M, Bernacchia A, Rugarli EI, Langer T. The m-AAA protease defective in hereditary spastic paraplegia controls ribosome assembly in mitochondria. *Cell*. 2005; 123(2):277.10.1016/j.cell.2005.08.003 [PubMed: 16239145]
9. Wright G, Terada K, Yano M, Sergeev I, Mori M. Oxidative stress inhibits the mitochondrial import of preproteins and leads to their degradation. *Exp Cell Res*. 2001; 263(1):107.10.1006/excr.2000.5096 [PubMed: 11161710]
10. Haynes CM, Petrova K, Benedetti C, Yang Y, Ron D. ClpP mediates activation of a mitochondrial unfolded protein response in *C. elegans*. *Dev Cell*. 2007; 13(4):467.10.1016/j.devcel.2007.07.016 [PubMed: 17925224]
11. Labrousse AM, Zappaterra MD, Rube DA, van der Blik AM. *C. elegans* dynamin-related protein DRP-1 controls severing of the mitochondrial outer membrane. *Mol Cell*. 1999; 4(5):815. [PubMed: 10619028]
12. Ades IZ, Butow RA. The transport of proteins into yeast mitochondria. Kinetics and pools. *J Biol Chem*. 1980; 255(20):9925. [PubMed: 6448842]
13. Feng J, Bussièrè F, Hekimi S. Mitochondrial electron transport is a key determinant of life span in *Caenorhabditis elegans*. *Dev Cell*. 2001; 1(5):633. [PubMed: 11709184]
14. Rowley N, Prip-Buus C, Westermann B, Brown C, Schwarz E, Barrell B, et al. Mdj1p, a novel chaperone of the DnaJ family, is involved in mitochondrial biogenesis and protein folding. *Cell*. 1994; 77(2):249. [PubMed: 8168133]

15. Oliveira RP, Abate J Porter, Dilks K, Landis J, Ashraf J, Murphy CT, et al. Condition-adapted stress and longevity gene regulation by *Caenorhabditis elegans* SKN-1/Nrf. *Aging Cell*. 2009; 8(5):524.10.1111/j.1474-9726.2009.00501.x [PubMed: 19575768]
16. Nakai K, Horton P. PSORT: a program for detecting sorting signals in proteins and predicting their subcellular localization. *Trends Biochem Sci*. 1999; 24(1):34. [PubMed: 10087920]
17. Braeckman BP, Houthoofd K, De Vreese A, Vanfleteren JR. Assaying metabolic activity in ageing *Caenorhabditis elegans*. *Mech Ageing Dev*. 2002; 123(2–3):105. [PubMed: 11718805]
18. Kennedy S, Wang D, Ruvkun G. A conserved siRNA-degrading RNase negatively regulates RNA interference in *C. elegans*. *Nature*. 2004; 427(6975):645.10.1038/nature02302 [PubMed: 14961122]
19. Suzuki CK, Suda K, Wang N, Schatz G. Requirement for the yeast gene LON in intramitochondrial proteolysis and maintenance of respiration. *Science*. 1994; 264(5161):891. [PubMed: 8178144]
20. Hill AA, Hunter CP, Tsung BT, Tucker-Kellogg G, Brown EL. Genomic analysis of gene expression in *C. elegans*. *Science*. 2000; 290(5492):809. [PubMed: 11052945]
21. Zhong M, Niu W, Lu ZJ, Sarov M, Murray JI, Janette J, et al. Genome-wide identification of binding sites defines distinct functions for *Caenorhabditis elegans* PHA-4/FOXA in development and environmental response. *PLoS Genet*. 2010; 6(2):e1000848.10.1371/journal.pgen.1000848 [PubMed: 20174564]
22. Benedetti C, Haynes CM, Yang Y, Harding HP, Ron D. Ubiquitin-like protein 5 positively regulates chaperone gene expression in the mitochondrial unfolded protein response. *Genetics*. 2006; 174(1):229.10.1534/genetics.106.061580 [PubMed: 16816413]

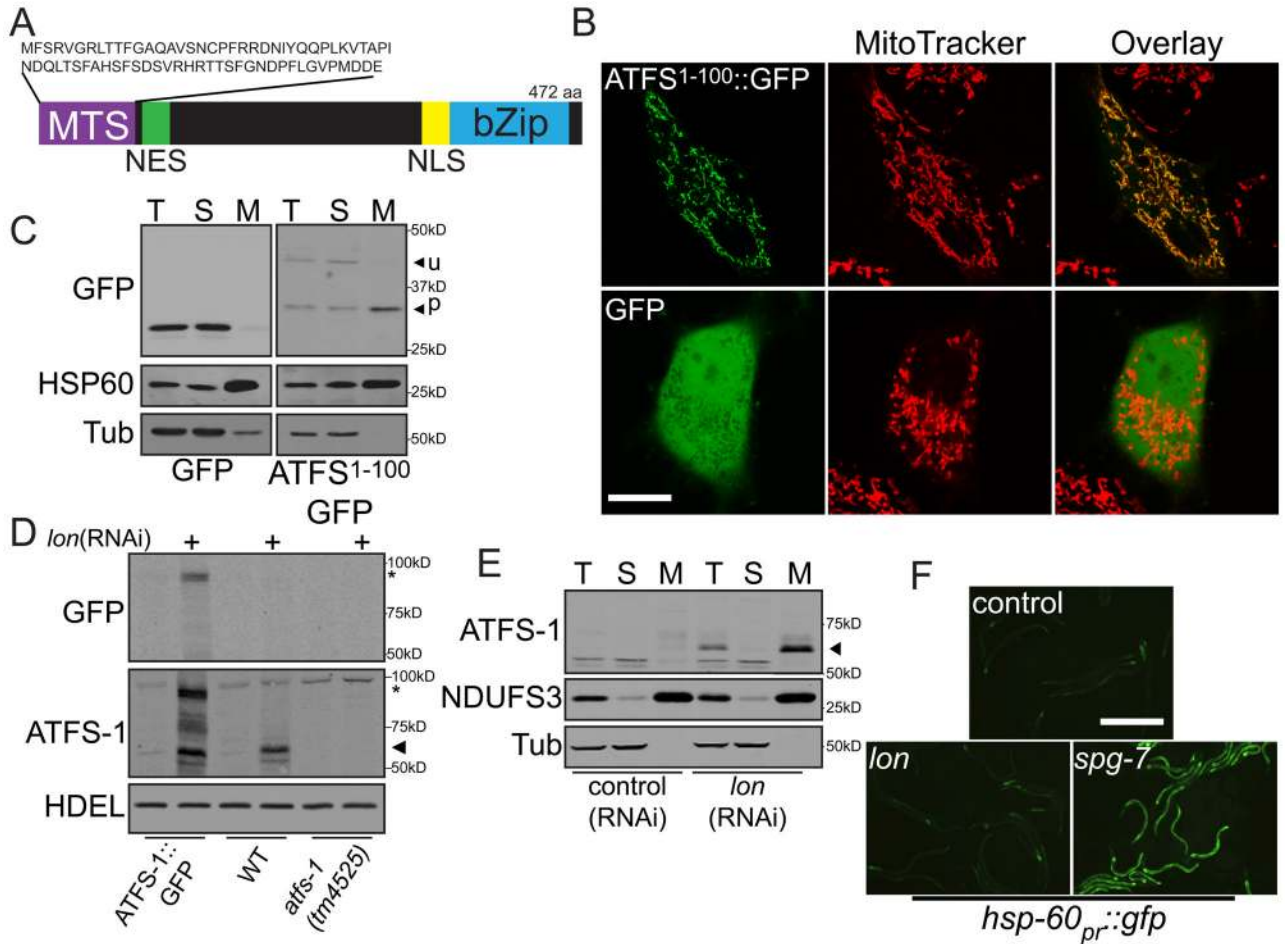


Figure 1. In the absence of stress, ATFS-1 is imported into mitochondria and degraded
A. ATFS-1 schematic.
B. Photomicrographs of HeLa cells expressing ATFS-1¹⁻¹⁰⁰::GFP or GFP stained with MitoTracker. Scale bar, 0.25 mm.
C. Immunoblots of HeLa cells expressing GFP or ATFS-1¹⁻¹⁰⁰::GFP following fractionation into total lysate (T), postmitochondrial supernatant (S) and mitochondrial pellet (M). Longer exposure of the ATFS-1¹⁻¹⁰⁰::GFP panel was required due to toxicity and weak expression.
D. Immunoblots of *atfs-1_{pr::atfs-1::gfp}*, wild-type or *atfs-1(tm4525)* worms raised on control or *lon*(RNAi). ATFS-1 (▶) and ATFS-1::GFP (*) are marked.
E. Immunoblots of wild-type worms fed control or *lon*(RNAi) following cellular fractionation. Endogenous NDUFS3 serves as a mitochondrial marker and α-tubulin as a cytosolic marker.
F. Photomicrographs of *hsp-60_{pr}::gfp* transgenic worms raised on control, *lon* or *spg-7*(RNAi). Scale bar, 0.5 mm.

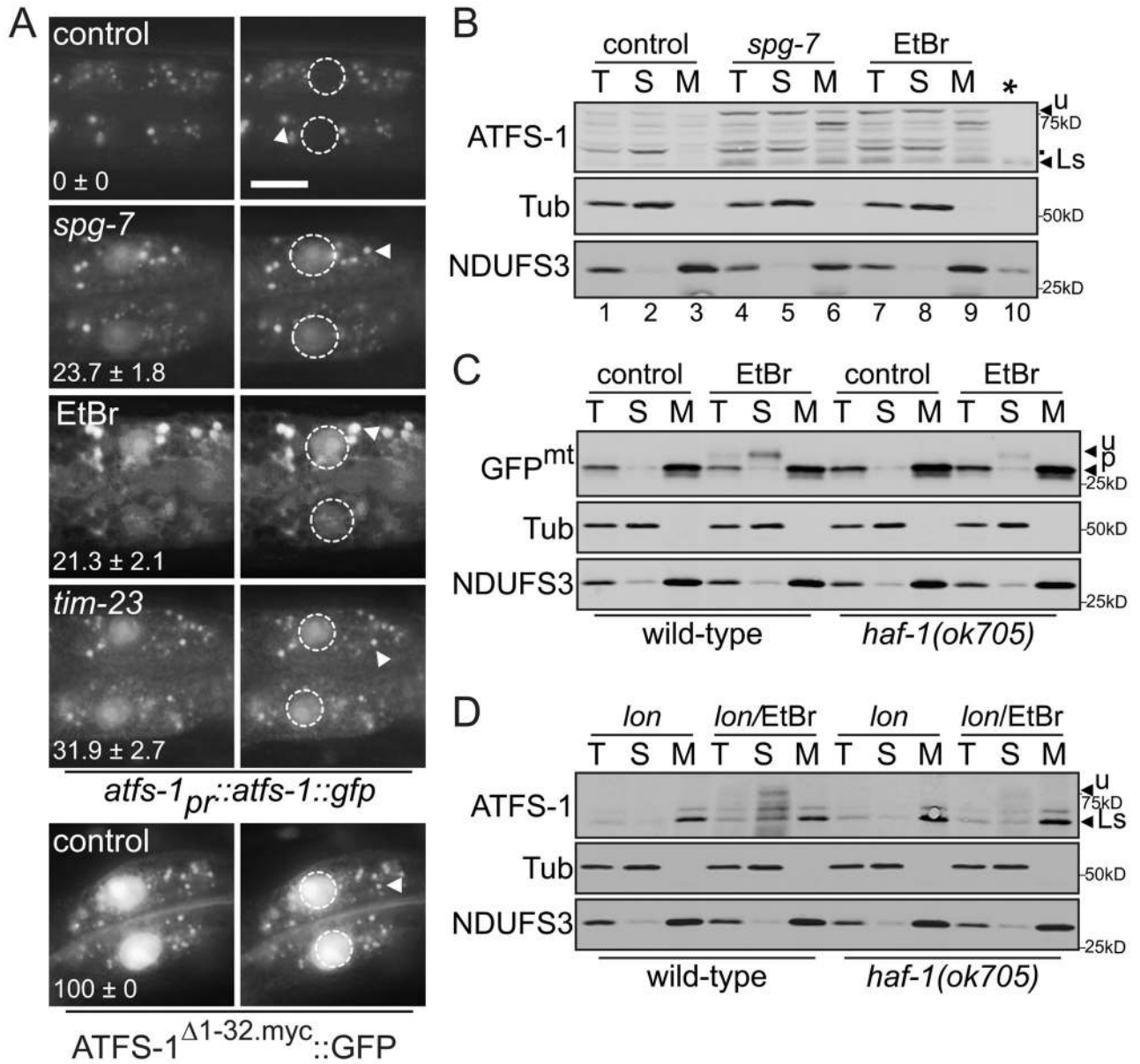


Figure 2. In the presence of mitochondrial stress, unprocessed ATFS-1 accumulates in nuclei
A. Photomicrographs of two intestinal cells in *atfs-1_{pr}::atfs-1::gfp* or *hsp-16_{pr}::atfs-1^{Δ1-32.myc}::gfp* transgenic animals raised on control, *spg-7* or *tim-23*(RNAi) or 100 μg/ml EtBr with the nuclei outlined (right panels). The punctae (arrowhead) are endogenous autofluorescence from intestinal cell lysosomes. The mean percentage ± SEM of worms with nuclear accumulation of ATFS-1::GFP is indicated (N = 3). Scale bar, 15 μm.
B. Immunoblots of fractionated lysates from wild-type worms raised on control, *spg-7*(RNAi) or EtBr (100 μg/ml). Lanes 1–9 are 100 μg from the described fractions and lane 10 (*) is 3 μg from the mitochondrial pellet of worms raised on *lon*(RNAi) for size comparison. Unprocessed and *lon*(RNAi) stabilized (Ls) ATFS-1 are indicated as are non-specific bands (.).
C. Immunoblots of fractionated extracts from wild-type or *haf-1(ok705)* worms raised on control(RNAi) in the absence or presence of 30 μg/ml EtBr expressing *hsp-16_{pr}::gfp^{mt}*.

D. Immunoblots of fractionated extracts from wild-type or *haf-1(ok705)* worms raised on *lon*(RNAi) in the absence or presence of 30 μ g/ml EtBr expressing *hsp-16_{pr}::atfs-1^{FL}*.

\$watermark-text

\$watermark-text

\$watermark-text

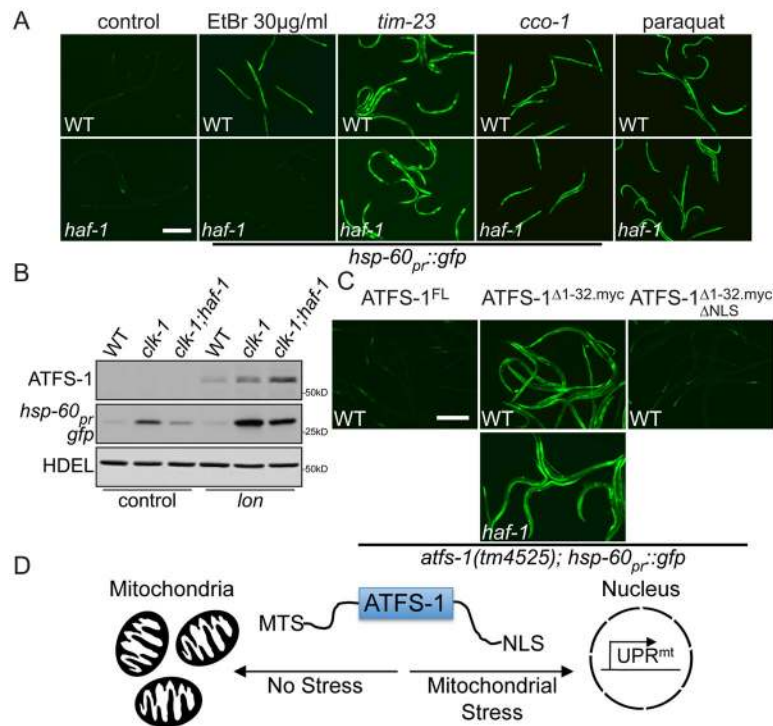


Figure 3. HAF-1 modulates UPR^{mt} signaling by slowing mitochondrial import of ATFS-1
A. Photomicrographs of wild-type and *haf-1(ok705); hsp-60_{pr}::gfp* worms raised on control, *tim-23*, *cco-1*(RNAi), EtBr or 0.5 mM paraquat. Scale bar, 0.5 mm. The images for *cco-1*(RNAi) and paraquat were exposed longer because of smaller worm size.
B. Immunoblots of wild-type, *clk-1(qm30)* or *clk-1(qm30); haf-1(ok705)* worms raised on control or *lon*(RNAi).
C. Photomicrographs of *atfs-1(tm4525); hsp-60_{pr}::gfp* worms expressing wild-type (^{FL}) ATFS-1, ATFS-1^{Δ1-32.myc} or ATFS-1^{Δ1-32.myc ΔNLS} raised on control(RNAi). The lower panel harbors the *haf-1(ok705)* allele. Scale bar, 0.5 mm.
D. Schematic illustrating ATFS-1 regulation.

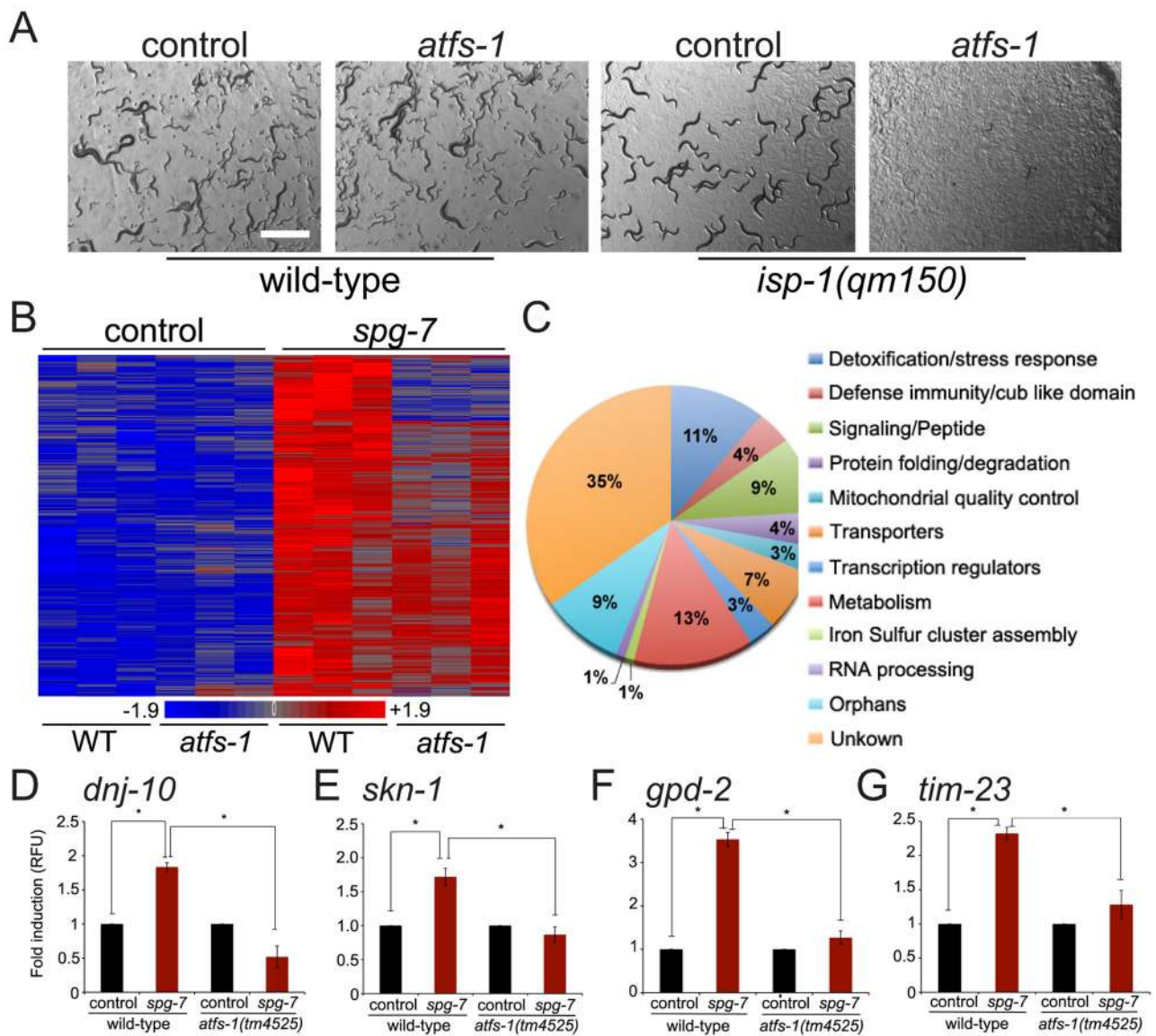


Figure 4. ATFS-1 mediates a broad and protective transcriptional program

A. Representative photomicrographs of wild-type or *isp-1(qm150)* worms raised on control or *atfs-1*(RNAi). Scale bar, 1mm.

B. Heat map comparing gene expression patterns of wild-type or *atfs-1(tm4525)* worms raised on control or *spg-7*(RNAi).

C. Functional categories of the 391 ATFS-1-dependent genes identified by hierarchical clustering.

D–G. Expression levels of *dnj-10*, *skn-1*, *gpd-2*, and *tim-23* mRNA in wild-type or *atfs-1(tm4525)* worms raised on control or *spg-7*(RNAi) determined by qRT-PCR (N = 3, ± SD, p* (student t-test) < 0.05).